# Journal Pre-proof


Core-shell type-II spherical quantum dot under externally applied electric field

V.A. Holovatsky, M.V. Chubrei, C.A. Duque

PII: S0040-6090(22)00062-1
DOI: https://doi.org/10.1016/j.tsf.2022.139142
Reference: TSF 139142

To appear in: *Thin Solid Films*

Received date: 4 December 2021
Revised date: 3 February 2022
Accepted date: 14 February 2022

Please cite this article as: V.A. Holovatsky, M.V. Chubrei, C.A. Duque, Core-shell type-II spherical quantum dot under externally applied electric field, *Thin Solid Films* (2022), doi: https://doi.org/10.1016/j.tsf.2022.139142

## HIGHLIGHTS

- Electron, hole, and exciton states in type-II core/shell spherical quantum dots
- Electron-hole interaction, overlap integral, and exciton lifetime are reported
- The applied electric field shifts the energy levels in the coating shell
- Higher energy transitions are independent of the electric field strength
- The electric field increases the radiative lifetime of the excitonic states

# Core-shell type-II spherical quantum dot under externally applied electric field

V. A. Holovatsky,[1] M. V. Chubrei,[1] and C. A. Duque[2]
[1] *Chernivtsi National University after Yuriy Fedkovych, Chernivtsi, Ukraine and*
[2] *Grupo de Materia Condensada-UdeA, Instituto de Física, Facultad de Ciencias Exactas y Naturales, Universidad de Antioquia UdeA, Calle 70 No. 52-21, Medellín, Colombia*

(Dated: February 16, 2022)

This study presents a simple one-band model within the effective mass approximation to describe the electric field impact on the energy structure and interband electron quantum transitions in type-II CdSe/ZnTe and ZnTe/CdSe spherical quantum dots. The dependencies of the oscillation strength and the light absorption coefficient on the externally applied electric field are calculated by the diagonalization method for spherical quantum dots of different sizes. It is shown that in the absence of an electric field and due to the spherical symmetry of nanosystem, only quantum transitions with $\Delta l = 0$ ($1s_e - 1s_h$, $1p_e - 1p_h$, $1d_e - 1d_h$, $1s_e - 2s_h$,...) are allowed. The oscillator strength of quantum transitions between electron and hole excited states is greater than between the ground states. The electric field breaks the spherical symmetry, therefore, the oscillator strength of the $1s_e - 1p_h$, $1s_e - 1p_h$, $1s_e - 1d_h$,... quantum transitions, which are forbidden for spherical symmetric systems, increase when electric field strength grows. Under electric field effects, the oscillator strength of allowed $\Delta l = 0$ quantum transitions decreases. Finally, we observed that the absorption peaks in the quantum dot spectra under electric field influence are shifted to the low-energy region.

Keywords: Type-II quantum dots; oscillator strength; exciton energy; interband transition; electric field; diagonalization method



## I. INTRODUCTION

The colloidal core-shell quantum dots (QDs) are heterostructures obtained by cheap chemical synthesis technologies. The atom-like spectrum of these nanostructures can be changed by tuning the core size and shell thickness. The core size and shell thickness control the physical properties of such nanostructures. The bandgap of the semiconductor material defines the maximal wavelength of the light emitted by electron interband transitions in QDs. There are not many semiconductor materials to obtain QDs operating in the infrared (IR) region [1]. With the help of doping, it is possible to achieve the infrared region for many materials.

"In type-II QDs, both the conduction and valence bands have higher energy in one material than in the other. Thus, one carrier type (electron or hole) is mainly confined to the core while the other is mainly confined to the shell. This spatial separation of carriers can produce properties that are quite different from those of type-I QDs. Type-II QDs can be prepared to emit at near-IR wavelengths using materials with bandgaps that are too wide to provide near-IR emission in a type-I QD structure. Typical Cd-based type-II QDs include CdSe/CdTe and CdSe/ZnTe core-shell QDs, which exhibit near-IR (NIR) emission due to electron-hole recombination across the core-shell interface" [1].

At type-II QDs, the interband absorption energy is less than the bandgap of any of the constituent semiconductors. Results of the experimental investigation related to photoluminescence spectra in core-shell CdTe/CdSe and ZnSe/ZnTe QDs [2] suggest the significant shift of the emission energy to the IR region spectra compared to the spectra of isolated CdTe and ZnSe QDs without shells. Such features of type-II QDs are proposed to be used as a sensitizer in solar concentrators for absorption of the full solar spectrum by solar cells, which will significantly improve their efficiency [3–5].

Spectroscopic properties of the core-shell structured type-II ZnTe/CdSe nanocrystals have been systematically studied by Long *et al.* [6]. In this study, it was found that the increase in radiation time with increasing shell thickness and core radius is explained by the separation of charges. In Ref. [7], the authors report about a 4-fold increasing average radiative lifetime of CdSe/ZnTe core-shell QDs compared to CdSe core, which suggests the spatial separation between the electron and hole in core-shell regions. Theoretical study of the interband quantum transitions energies in QDs of the second type —ZnTe/ZnSe [8], CdSe/ZnTe [9, 10], ZnTe/CdSe [11], CdTe/CdSe, and CdSe/CdTe [12–14]— is performed mainly by the effective mass method. In these studies, the influence of geometric parameters (design) of QDs on the energy spectrum and electron and a hole wavefunctions have been investigated. On this basis, the energies and forces of the oscillator of interband quantum transitions were calculated. Only quantum transitions allowed by the selection rules for spherically symmetric nanosystems were considered. Even in Ref. [9], where the influence of the electric field on the energy spectrum was

studied, only the transitions between the ground states of quasiparticles were taken into account. The influence of an electric field on the energy spectrum of electrons in type-I QD was studied by different methods: analytically for a particular case [15], configuration-integration methods [16], finite element method [17], and matrix method [18–22]. The combined effects of hydrostatic pressure and temperature on the nonlinear properties of an exciton in a GaAs/GaAlAs spherical QD under the applied electric field have been reported by Lu *et al.* [24]. In their work, the authors used a parabolic confinement potential model and the perturbation method to obtain the correction term of the energy associated with the Coulomb interaction.

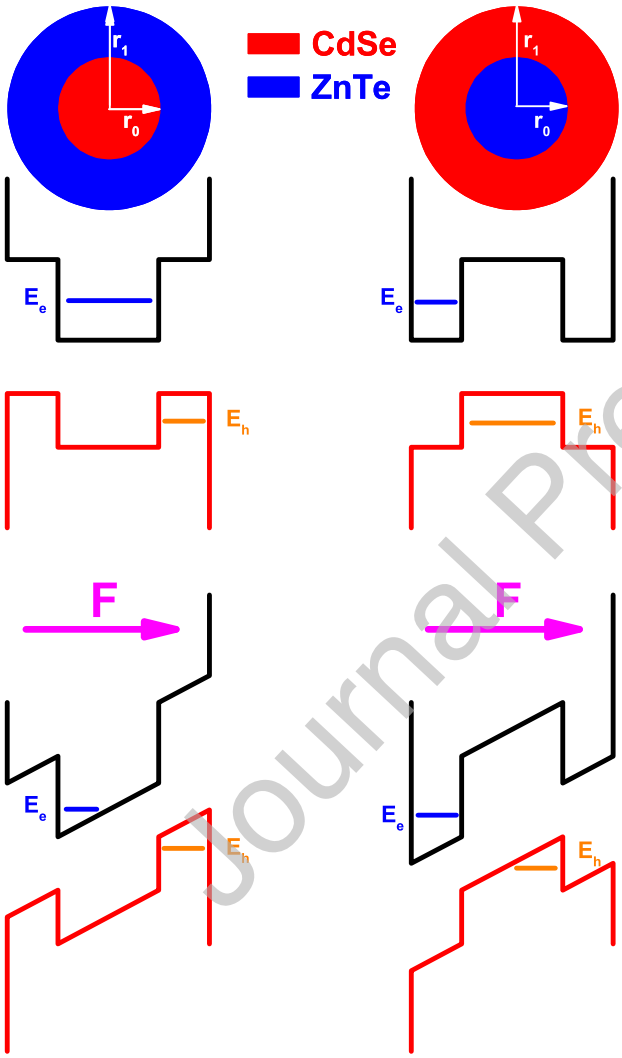


FIG. 1. (color online) The $x$-dependence of the electron and hole confinement potentials in CdSe/ZnTe (left hand column) and ZnTe/CdSe (right hand column) quantum dots without (upper part) and with (lower part) $x$-directed applied electric field. The electron and hole ground state energies are illustrated.

The electric field breaks the spherical symmetry of the 3D-spherical QDs, and thus, the rules for selecting quantum transitions, valid for spherical nanosystems, become invalid. Under the influence of the electric field, the new states of quasiparticles do not have a particular value of the orbital quantum number, but they are a superposition of states with different values. So, to study the effects of the electric field on the optical properties of nanosystems, it is necessary to consider all possible quantum transitions, considering that only the ground states of quasiparticles are insufficient. Such studies for type-II QD are performed in this paper. The paper's organization is the following: Section II contains the presentation of the theoretical framework, in Section III, we discuss the obtained results, and in Section IV, the conclusions are given.

## II. THEORETICAL FRAMEWORK

The type-II CdSe/ZnTe QD is considered, the geometric scheme and the scheme of potential energy electron and hole in nanosystem are shown in Fig. 1.

The Schrödinger equation for confined electron (hole) in core-shell CdSe/ZnTe or ZnTe/CdSe QDs under $x$-directed applied electric field ($x = r\,\cos\theta$) is given by

$$H_{e(h)}\,\Psi^{jm}_{e(h)}(\vec{r}) = E^{jm}_{e(h)}\,\Psi^{jm}_{e(h)}(\vec{r})\,, \tag{1}$$

where the Hamiltonian $H_{e(h)}$ has the form

$$H_{e(h)} = -\frac{\hbar^2}{2}\vec{\nabla}\cdot\left(\frac{1}{m^*_{e(h)}(r)}\vec{\nabla}\right) \mp e\,F\,r\,\cos\theta + U_{e(h)}(r)\,, \tag{2}$$

where $e$ is the absolute value of the electron charge and $F$ is the electric field strength. The negative (positive) sign of the second term at the right hand side of the Eq. (2) corresponds to the electron (hole). The terms $m^*_i$ and $U_i$ (with $i = e, h$) are the carrier effective mass and confinement potential. In the case of the CdSe/ZnTe QDs, the electron (hole) confinement potential is given by $U_e(r) = 0$ ($U_h(r) = V_h$) for $r \le r_0$, $U_e(r) = V_e$ ($U_h(r) = 0$) for $r_0 < r \le r_1$, and $U_e(r) \to \infty$ ($U_h(r) \to \infty$) for $r > r_1$, whereas for the ZnTe/CdSe the confinement potential is $U_e(r) = V_e$ ($U_h(r) = 0$) for $r \le r_0$, $U_e(r) = 0$ ($U_h(r) = V_h$) for $r_0 < r \le r_1$, and $U_e(r) \to \infty$ ($U_h(r) \to \infty$) for $r > r_1$. In our calculations, we consider the position dependent effective mass, i.e., we consider the appropriate values of the electron (or hole) effective mass in the CdSe and ZnTe semiconductor materials.

In order to study the electron and hole properties in nanosystem driven by electric field, we are going to use the expansion method for the quasiparticle wavefunction by using the complete set of electron and hole eigenfunctions in the spherical nanostructure without the external field ($\Phi^{nlm}_{e(h)}(\vec{r})$), they are obtained as the exact solutions of the Schrödinger equation. When the external electric

field is turned on, the spherical symmetry of the problem is broken and the $l$-orbital quantum number becomes not convenient. The new states characterized by a $m$-magnetic quantum number are represented as a linear combination of the $\Phi^{nlm}_{e(h)}(\vec{r})$ states

$$\Psi^{jm}_{e(h)}(\vec{r}) = \sum_n \sum_l c^{jnlm}_{e(h)} \Phi^{nlm}_{e(h)}(\vec{r})\,. \tag{3}$$

Due to the spherical symmetry of the problem, the electron (or hole) wavefunction will take the form $\Phi^{nlm}_{e(h)}(\vec{r}) = R^{nl}_{e(h)}(r)\, Y_{lm}(\theta,\phi)$, where $Y_{lm}(\theta,\phi)$ are the spherical harmonic functions, and the $R^{nl}_{e(h)}(r)$ radial functions are a linear combination of the $j_l$ and $n_l$ Bessel functions of the first and second kind, respectively [23]. Taking to account the large band gap of external medium (vacuum), the Dirichlet boundary conditions can be applied, i.e., $R^{nl}_{e(h)}(r_1) = 0$. The electron (and hole) energies without electric field effects, $E_{e(h)0}$, are obtained by imposing the Ben Daniel-Duke boundary conditions at $r = r_0$.

To determine the expansion coefficients $c^{jnlm}_{e(h)}$ in Eq. (3) and the quasiparticle energy spectra $E^{jm}_{e(h)}$ in Eq. (1), we have to solve the secular equation

$$\left| H^{n'l',nl}_{e(h)} - E^{jm}_{e(h)}\, \delta_{n,n'}\, \delta_{l,l'} \right| = 0\,. \tag{4}$$

Here, the matrix elements $H^{nl,n'l'}$ have the form

$$H^{n'l',nl}_{e(h)} = E^{nl}_{e(h)0}\, \delta_{n',n}\, \delta_{l',l} \mp e\,F\, (\alpha_{l,m}\, \delta_{l,l+1} + \beta_{l,m}\, \delta_{l,l-1})\, U^{n'l',nl}\,, \tag{5}$$

where

$$\alpha_{l,m} = \sqrt{\frac{l^2-(m+1)^2}{(2\,l+3)(2\,l+1)}}\,, \tag{6}$$

$$\beta_{l,m} = \sqrt{\frac{l^2-m^2}{4\,l^2-1}}\,, \tag{7}$$

and

$$U^{n'l',nl}_{e(h)} = \int_0^{r_2} r^3\, R^{n'l'}_{e(h)}(r)\, R^{nl}_{e(h)}(r)\, dr\,. \tag{8}$$

The quasiparticles spectra and wavefunctions in nanosystem driven by uniform electric field are completely defined by the obtained eigenvalues, $E^{jm}_{e(h)}$, and eigenvectors, $c^{jnml}_{e(h)}$, of $H^{n'l',nl}$ matrix for each $m$. Herein, the new functions $\Psi^{jm}_{e(h)}(\vec{r})$ , with the fixed value of magnetic quantum number, are obtained from the expansion in Eq. (3), over the wavefunctions $\Phi^{nlm}_{e(h)}(\vec{r})$ with the same $m$. The electron and hole states are characterized by two $j$ and $m$ quantum numbers. Here, $j$ denotes the number of the energy level at fixed $m$. For convenience, we will denote in graphics the new states by the $l$-index, which corresponds to the orbital quantum number of the non-perturbed wavefunction. The notation $1s$, $1p$,... is valid only at $F = 0$. We are using such atomic notation for convenience in order to have visual information about selection rules for optical transitions.

The electron-hole Coulomb interaction energy between the $i$ and $f$ states is given, in effective Rydberg units, by the following Coulomb integral

$$E^{if}_b = \frac{2}{\varepsilon} \int_{\Omega_h} \int_{\Omega_e} \frac{\left|\Psi^{ex}_{if}(\vec{r}_e,\vec{r}_h)\right|^2}{|\vec{r}_e - \vec{r}_h|} d^3\vec{r}_e\, d^3\vec{r}_h\,, \tag{9}$$

where $\Psi^{ex}_{if}(\vec{r}_e,\vec{r}_h) = \Psi^i_e(\vec{r}_e)\, \Psi^f_h(\vec{r}_h)$, $\varepsilon = \sqrt{\varepsilon_{\rm CdSe}\, \varepsilon_{\rm ZnTe}}$ is average dielectric constant, and $\Omega_e$ ($\Omega_h$) indicates the integration volume for the electron (hole), which in this case runs over the QD volume. Since the magnetic quantum number taken is zero, therefore the $m$-index was omitted. The effective Rydberg ($R_0$) and effective Bohr radius ($a_0$) were taken to be the energy and length units, respectively, in Eq. (9).

The oscillator strengths of the interband quantum transitions defines the strength of absorption lines, and can be obtained via the expression [16]

$$f_{if} = \frac{E_p}{2\,E^{if}} \left| \int_\Omega \Psi^{e*^3}_i(\vec{r})\, \Psi^h_f(\vec{r})\, d^3\vec{r} \right|^2\,, \tag{10}$$

where $E_p$ and $E^{if} = E_g + E^{j0}_e + E^{j0}_h - E^{if}_b$ are the Kane and interband transition energies, respectively. Here, $E_g = E_g^{\rm CdSe} - V_h = E_g^{\rm ZnTe} - V_e$ is the effective energy gap between the bottom of the CdSe conducting band and the top of the ZnTe valence band (indirect bandgap).

The radiative lifetime is another important quantity in both theoretical and experimental investigations of the excitonic structures [7, 14, 25–27]. The oscillator strength $f_{if}$ defines the strength of absorption lines and also relates to the radiative lifetime, $\tau$, which is given by [27]

$$\tau_{if} = \frac{6\,\pi\,\varepsilon_0\, m_0\, c^3\, \hbar^2}{e^2\, n\, f_{if}\, (E^{if})^2}\,, \tag{11}$$

where $\varepsilon_0$ is the dielectric permittivity of the vacuum, $m_0$ is the free electron mass, $c$ is the light velocity in the vacuum, $e$ is the bare electronic charge, $f_{if}$ is the oscillator strength, $n$ is the refractive index of QD material, and $E^{if}$ is the transition energy of considered system.

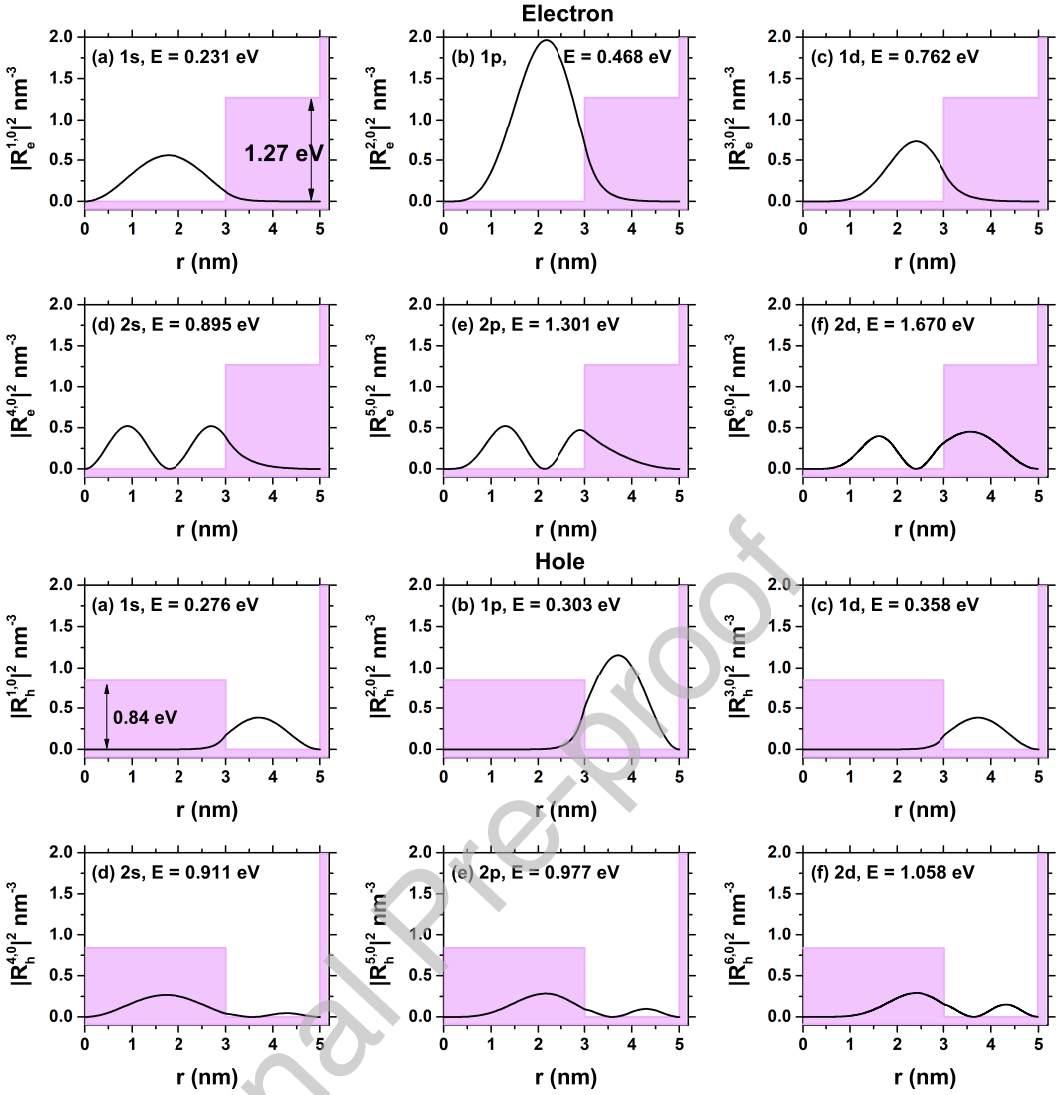


FIG. 2. (color online) Electron and hole radial distribution of probability densities ($|R^{nl}_{e(h)}|^2$) corresponding to the normalized wavefunction in CdSe/ZnTe QDs. The notation $1s$, $1p$,... is valid only at $F = 0$. We are using such atomic notation for convenience in order to have visual information about selection rules for optical transitions.

## III. RESULTS AND DISCUSSION

In our numerical calculations for electron, hole and exciton states, with their corresponding properties, confined in CdSe/ZnTe and ZnTe/CdSe spherical QDs we have used the following physical parameters [9]: *i*) CdSe: $m^*_e = 0.13\,m_0$, $m^*_h = 0.45\,m_0$, $E_g = 1.75\,\text{eV}$, and $\varepsilon = 10.6$; *ii*) ZnTe: $m^*_e = 0.15\,m_0$, $m^*_h = 0.2\,m_0$, $E_g = 2.2\,\text{eV}$, and $\varepsilon = 9.7$; *iii*) $r_0 = 3\,\text{nm}$, $r_1 = 5\,\text{nm}$, $V_e = 1.27\,\text{eV}$, and $V_h = 0.84\,\text{eV}$.

In Fig. 2, the radial distributions of probability densities corresponding to the normalized wavefunction for the electron and hole ($|R^{nl}_{e(h)}|^2$) in type-II CdSe/ZnTe QD for several lowest states are presented. At energy $E^{nl}_{e(h)0} < V_{e(h)}$, the electron (hole) is localized in the core (shell) region. In the case of the hole radial distribution of probability densities, the discontinuity of the derivative at $r = 3\,\text{nm}$ is quite evident, which is consistent with the Ben Daniel-Duke boundary conditions due to the wide difference that exists between the hole effective masses in the core and shell regions. Note the significant value of $|R^{2d}_e|^2$ ($|R^{2s}_h|^2$, $|R^{2p}_h|^2$, and $|R^{2d}_h|^2$) in the shell (core) region due to the fact that in that case the state energy exceeds the height of the potential barrier for the electron, $V_e$ (for the hole, $V_h$). For calculations where the influence of electric field has been considered, we used not less than 20 terms in the expansion given by Eq. (3) to guarantee the convergence of our calculations up to 0.01 meV.

In Fig. 3 the dependencies of the electron and hole

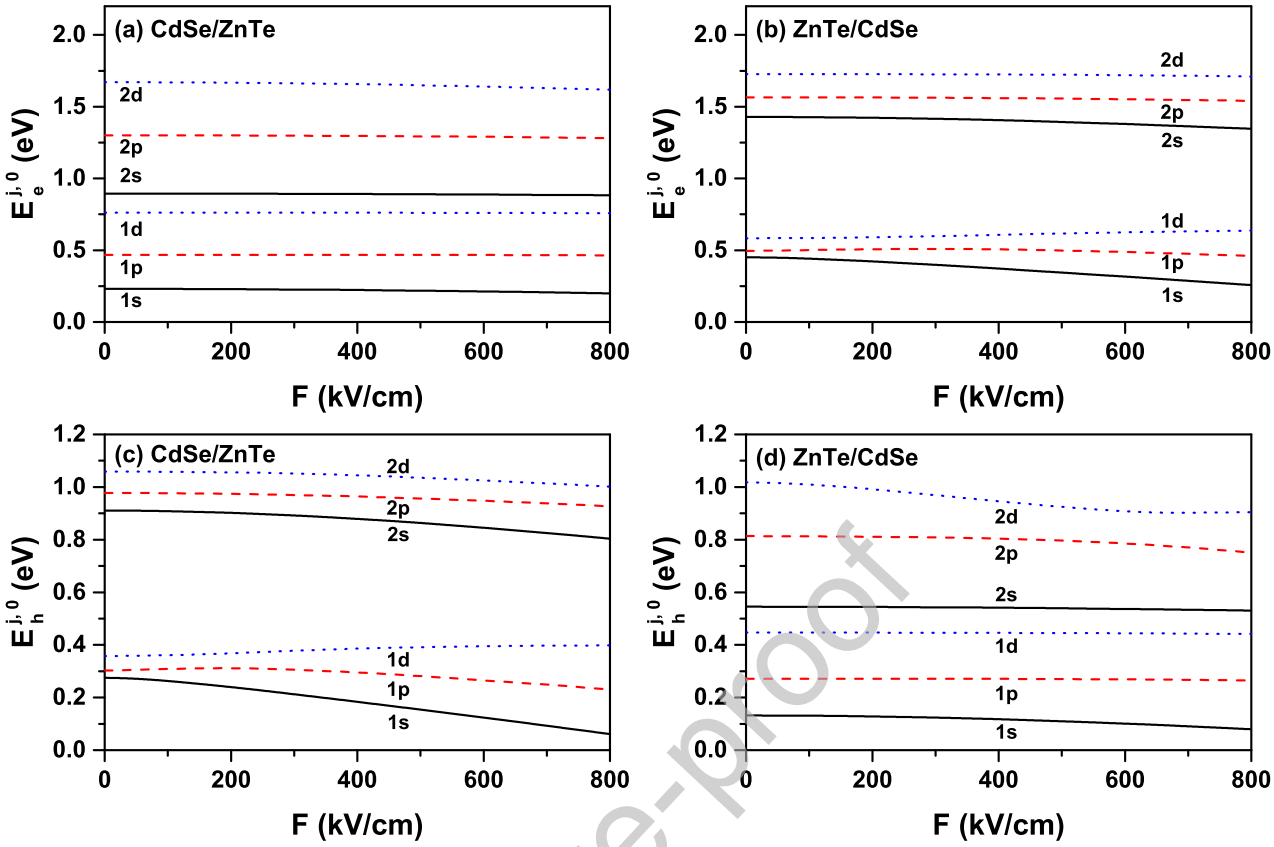


FIG. 3. (color online) Dependencies of the electron (a,b) and hole (c,d) energies on the applied electric field strength in CdSe/ZnTe (a,c) and ZnTe/CdSe (b,d) spherical quantum dots. All reported states are obtained with the magnetic quantum number equal to zero. The notation $1s$, $1p$,... is valid only at $F = 0$. We are using such atomic notation for convenience in order to have visual information about selection rules for optical transitions.



energies on the electric field strength in CdSe/ZnTe and ZnTe/CdSe QDs are shown. The figure proves that an increasing electric field intensity shifts the energy levels to a lower energy range (down). The shift value is greater for localized in-shell quasiparticles. When the charge carrier (electron or hole) is located mainly in the core region, a strong localization of the wavefunctions appears, and it becomes difficult to polarize the system as an effect of the electric field. This fact explains the reason why in Figs. 3(a) (for the electron) and 3(d) (for the hole), the energy curves are essentially constant with electric field strength. With the effective mass and dielectric constant parameters reported above, $a_0 = 4.3\,\text{nm}$ for the electron in CdSe and $a_0 = 2.6\,\text{nm}$ for the hole in ZnTe. Note that $r_0 = 0.69\,a_0$ for the electron confined in the CdSe/ZnTe QD while for the hole confined in the core of the ZnTe/CdSe we have $r_0 = 1.15\,a_0$.

In Fig.4, the dependencies of the interband transitions energies on the electric field strength for a confined electron-hole pair in CdSe/ZnTe and ZnTe/CdSE QDs are shown. The energy of the quantum transition between ground states of the quasiparticles, ($E_{1s-1s}$), corresponds to the near-infrared region of the spectrum. The energy of the next allowed quantum transitions, $E_{1p-1p}$, corresponds to the lower limit of the visible light range and at electric field strength $0.3\,\text{MV/cm}$ for the CdSe/ZnTe ($0.5\,\text{MV/cm}$ for the ZnTe/CdSe) QD goes down into infrared energy region. The highest allowed energy transition, $E_{1d-1d}$, is almost independent of electric field strength and belongs to the visible regime.

In Fig. 5 are presented our results for the interband transitions oscillator strength concerning the applied electric field strength for a confined electron-hole pair in CdSe/ZnTe (a,b) and ZnTe/CdSe (c,d) QDs. In Figs. 5(a,c) the calculations are for allowed transitions at $F = 0$, whereas in Figs. 5(b,d) are for the forbidden transitions at $F = 0$. When the electric field strength increases, the intensity of allowed interband quantum transitions decreases due to the decreasing of the quasiparticles wavefunctions overlap. It is suggested by Figs. 5(a) and 5(c), where the dependencies of the oscillator strength of the allowed interband transitions at $F = 0$ concerning the electric field strength are shown. Note in Figs. 5(a) and 5(c) that the oscillator strength for the $1s-1s$ transition is the least sensitive to variations in the electric field and that at zero electric field its magnitude

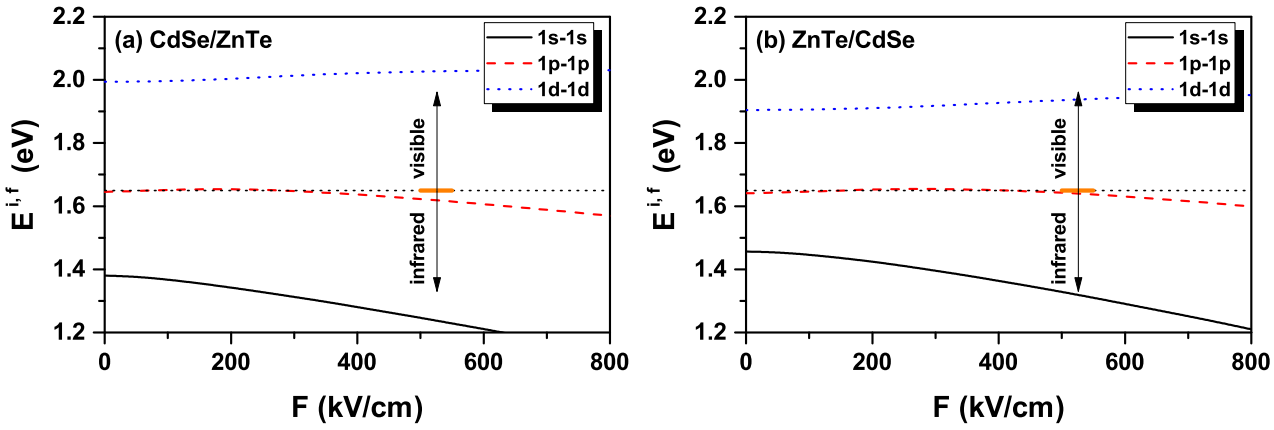


FIG. 4. (color online) Dependencies of the interband transitions energies on the electric field strength for a confined electron-hole pair in CdSe/ZnTe (a) and ZnTe/CdSe (b) quantum dots. The label $1s-1s$, for example, means the ground state both for electron and hole. The dotted line at 1.65 eV corresponds to the infrared-visible transition. The notation $1s$, $1p$,... is valid only at $F = 0$.

is less than that of the $1p-1p$ and $1d-1d$ transitions. It is clear that their ground states are located in their corresponding well regions for both the electron and the hole, favoring a very low overlap of the wavefunctions. As transitions between excited states are considered, the results in Fig. 2 show that the electron and hole wavefunctions present a greater penetration towards the regions of their corresponding potential barriers, thus favoring the increase in the overlap. This explains the reason why at $F = 0$ we have $f(1s-1s) < f(1p-1p) < f(1d-1d)$. The decreasing character of all the curves in Figs. 5(a) and 5(c) is justified by the fact that the electric field pushes the two charge carriers (electron and hole) in opposite space directions, giving rise to a decrease in the overlap between the wavefunctions. Note that the electric field breaks the even and odd symmetries of the electron and hole wavefunctions concerning the QD-center. This is why those transitions that are null due to the symmetry of the wavefunctions at zero electric field become allowed when the electric field is turned on, as shown in Figs. 5(b) and 5(d). Figs. 5(b) and 5(d) depict increasing of oscillator strength of forbidden interband transitions with grows electric field strength (FrankKeldysh effect [28]). First, they increase due to the violation of spherical symmetry and then decrease due to the reduction of the overlap of the wavefunctions. Those transitions that involve the ground state of one of the carriers with highly excited states of the other carrier, such as $1s-1d$ and $1d-1s$, are slightly sensitive to the effects of the electric field, as shown in Figs. 5(b) and 5(d). Note that even up to $F = 400\,\mathrm{kV/cm}$, the oscillator strength for these transitions does not reach a maximum, which is visible for the other transitions. This result is associated with the fact that the more extended a state is in QD space, the more difficult it is to modify its wavefunction due to the effect of the electric field.

In Fig. 6 are reported our results for the ground state exciton binding energy and exciton radius (average electron-hole distance) as a function of the electric field strength for a confined electron-hole pair in CdSe/ZnTe and ZnTe/CdSe QDs. In this case, both the electron and the hole are considered to be in their ground states. The results are closely connected with the curves denoted as $1s-1s$ in Figs. 5(a) and 5(c), where it was shown that as the applied electric field increases, the oscillator strength of the $1s-1s$ transition decreases. This is reflected in a decrease in the overlap between the electron and hole wavefunctions which finally translates into an increase in the average separation between the two charge carriers, as seen for the dashed lines in Fig. 6. By increasing the separation between carriers, the Coulomb interaction between them decreases, and therefore the binding energy decreases, a situation that can be seen for the solid lines in Fig. 6. In the CdSe/ZnTe structure, where the ground state of the electron (hole) is located in the shell (core) region, greater sensitivity of the average separation of the two charge carriers is observed concerning the applied electric field. This is associated with the fact that the electron is located in the region of greater volume and the system is much more polarizable concerning the situation in which the electron is located in the core and the hole in the shell region. In the latter case, for example, while the confinement volume for the electron is $36\,\pi\,\mathrm{nm}^3$, for the hole is $131\,\pi\,\mathrm{nm}^3$. The previous fact justifies that at a fixed value of the applied electric field, the binding energy for the ZnTe/CdSe system is lower than that corresponding to the CdSe/ZnTe one. By using a variational technique and the envelope function approximation, the binding energy and the mean distance between the electron and hole of an exciton inside a CdSe/ZnTe core/shell spherical QD was studied considering the dependence of the dielectric constant and charge carriers effective mass on radius [32]. For the case $r_0 = 9.6\,\mathrm{nm}$ and $r_1 = 16\,\mathrm{nm}$, the authors reported 85 meV and 0.16 nm for the binding

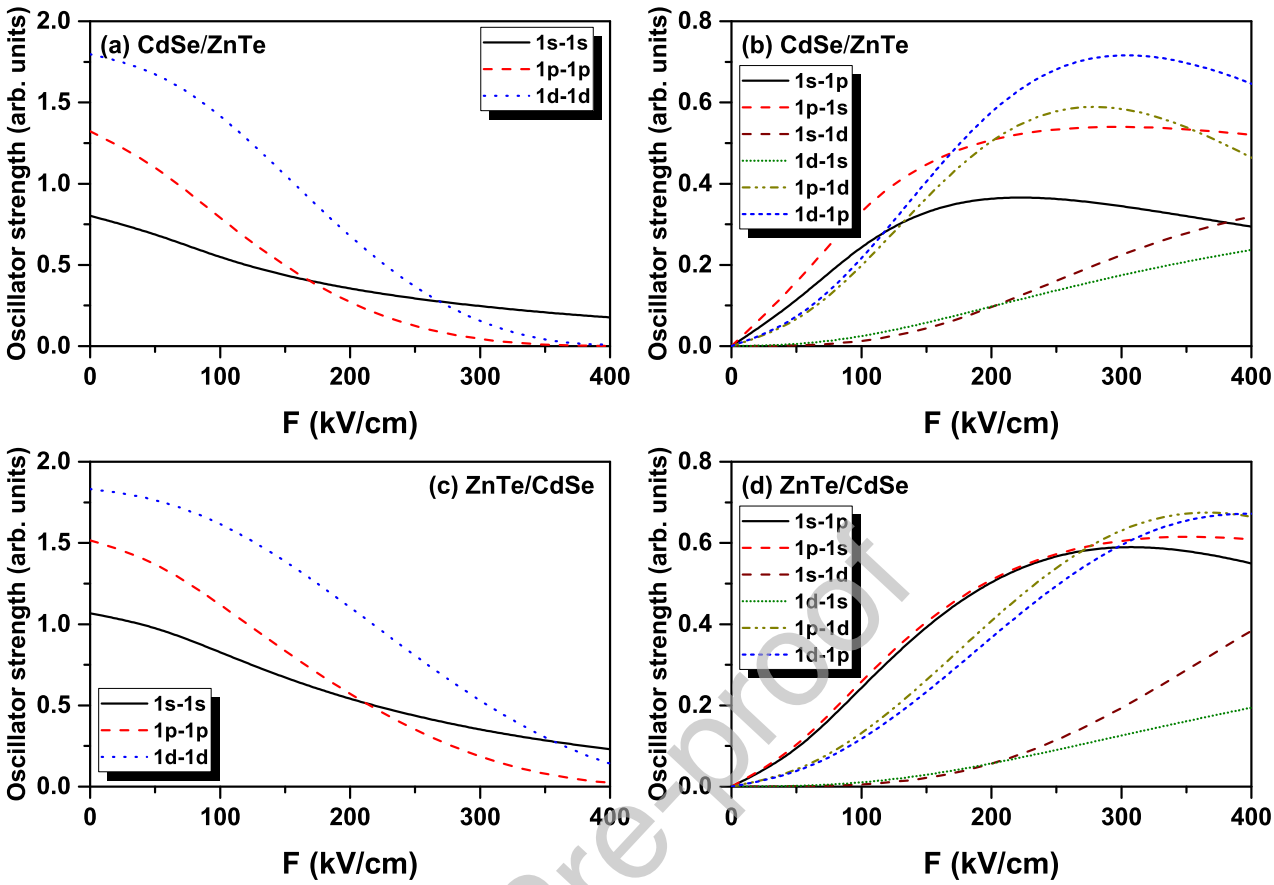


FIG. 5. (color online) Dependencies of the interband transitions oscillator strength on the applied electric field strength for a confined electron-hole pair in CdSe/ZnTe (a,b) and ZnTe/CdSe (c,d) QDs. In (a,c) the results are for allowed transitions at $F = 0$, whereas in (b,d) are depicted the forbidden transitions at $F = 0$. The label $1s - 1p$, for example, means the $1s$ state for electron and the $1p$ state for hole. The notation $1s$, $1p$,... is valid only at $F = 0$.

energy and average electron-hole distance, respectively. In this work, for the same CdSe/ZnTe QD structure, but for $r_0 = 3\,\text{nm}$, $r_1 = 5\,\text{nm}$, we obtained 38.96 meV and 4.03 nm for the binding energy and average electron-hole distance, respectively. Considering this important difference between both results, we have decided to implement the calculation of the binding energy for at least one of the structures studied and using another class of methods that can better account for the binding energy. Indeed, a first-order perturbative calculus can be quite crude as it does not take into account the effects of many mixed states. Following the work of Ref. [33], where a configuration interaction approach is used and the binding energy matches the experimental values, we have calculated the binding energy for the CdSe/ZnTe case with $r_0 = 3\,\text{nm}$ and $r_1 = 5\,\text{nm}$ finding a binding energy value of 50.0 meV, differing by 22% with respect to the values obtained perturbatively. This has allowed us to have a certain peace of mind regarding the value reported here. Additionally, considering that the electron and the hole are located in different spatial regions, the value of the average electron-hole distance that we have obtained seems

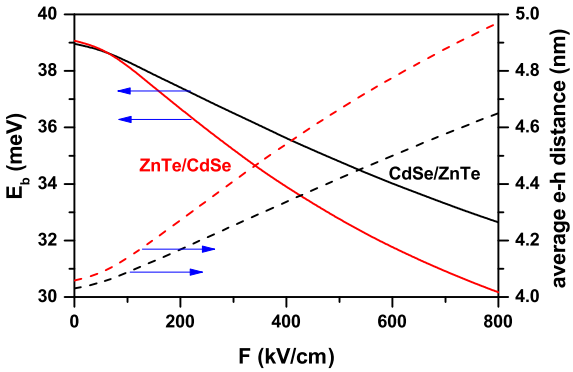


FIG. 6. (color online) Dependencies of the ground state exciton binding energy and exciton radius (average electron-hole distance) on the electric field strength for a confined electron-hole pair in CdSe/ZnTe and ZnTe/CdSe QDs.

quite satisfactory and in line with the value of the binding energy reported. Finally, we want to stress that our results very good agrees with results from Koc and Sahin [14] for CdSe/CdTe-based multi-shell type-II quantum

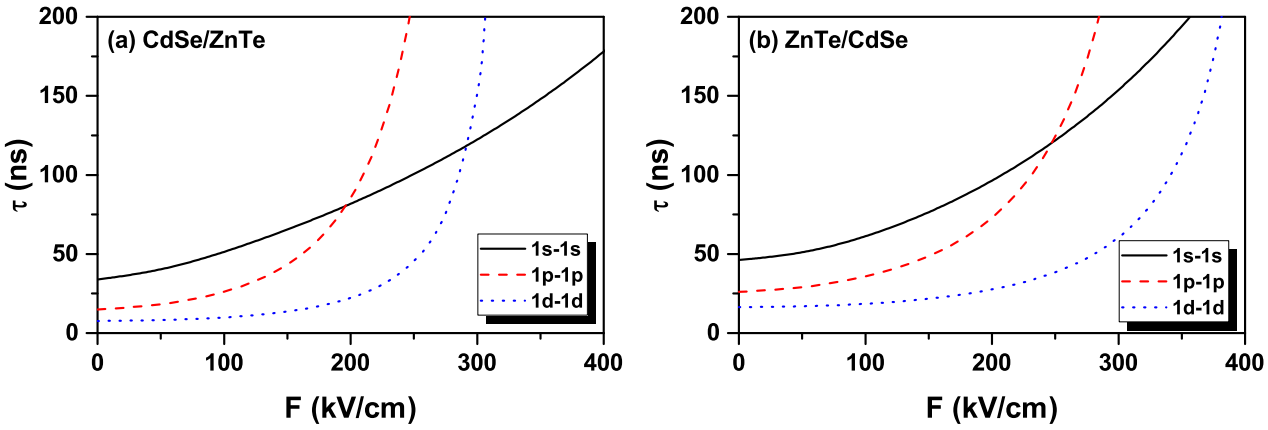


FIG. 7. (color online) Dependencies of the radiative time for interband transitions on the electric field strength for a confined electron-hole pair in CdSe/ZnTe (a) and ZnTe/CdSe (b) QDs. The notation $1s$, $1p$,... is valid only at $F = 0$.

dot ($r_0 = 1.95\,\text{nm}$).

In Fig. 7, we present our results for the radiative lifetime for interband transitions concerning the electric field strength for a confined electron-hole pair in CdSe/ZnTe (a) and ZnTe/CdSe (b) QDs. From Eq. (11), it is clearly inferred that the radiative lifetime is inversely proportional to both the oscillator strength and the transition energy. In this sense, the decreasing effect of the curves labeled as $1s-1s$, $1p-1p$, and $1d-1d$ in Figs. 5(a) and 5(c) combined with the decreasing or quasi-constant effect of the same three crows in Figs. 4(a) and 4(b) explain why in the two panels of Fig. 7, all the radiative lifetimes are increasing functions of the applied electric field. At zero field, the order in which the oscillator strengths and transition energies appear is the same inverse order in which the radiative lifetimes appear. Note that the changes in the transition energies with the applied electric field in Fig. 4 are essentially minimal for the $1p-1p$ and $1d-1d$ transitions and do not exceed 25% for the $1s-1s$ transition while Figs. 5(a) and 5(b) show a strong dependence on the applied electric field of the oscillator strength. The latter allows us to infer that the behavior shown by the radiative lifetime of the curves in Fig. 7 is completely dominated by the oscillator strength. The crosses observed between curves in Figs. 5(a) and 5(b) are replicated in Fig. 7. Clearly, the increase in the radiative lifetime allows us to conclude that the electric field favors the stability of the excitonic states confined in the QD.

## IV. CONCLUSIONS

The aim of this study is to investigate the effect of electric field on the interband transition in type-II spherical core-shell QD. We have studied the electric field effects on the energies and wavefunctions of the ground ($1s$) and excited ($1p$, $1d$, $2s$,... ) states of an electron and hole by matrix diagonalization method. On this base, the oscillator strength of interband transitions and exciton lifetime were calculated as a function of the electric field. The electric field reduces the intensity of the allowed quantum transitions and increases the intensity of the forbidden ones. The energies of quantum transitions between the lowest energy levels of electrons and holes are shifted to the low-energy region of the spectrum. The electric field increases the spatial separation of the charge carriers, which leads to an increase in the radiation time. This result is qualitatively consistent with the experimental data [2, 5–7, 29–31].

## CRediT authorship contribution statement

**V. A. Holovatsky:** Conceptualization, Methodology, Software, Validation, Formal analysis, Investigation, Writingoriginal draft, Writingreview & editing, Visualization, Supervision. **M. V. Chubrei:** Software, Validation, Formal analysis, Investigation, Writingoriginal draft. **C. A. Duque:** Validation, Formal analysis, Resources, Data curation, Writingreview & editing.

## Declaration of Competing Interest

The authors declare that they have no known competing financial interests or personal relationships that could have appeared to influence the work reported in this paper.

## Acknowledgments

The authors are grateful to the Colombian Agencies: CODI-Universidad de Antioquia (Estrategia de Sostenibilidad de la Universidad de Antioquia and projects "Propiedades magneto-ópticas y óptica no lineal en superredes de Grafeno", "Estudio de propiedades ópticas en sistemas semiconductores de dimensiones nanoscópicas",

and "Propiedades de transporte, espintrónicas y térmicas en el sistema molecular ZincPorfirina"), and Facultad de Ciencias Exactas y Naturales-Universidad de Antioquia (CAD exclusive dedication project 2021-2022). The authors also acknowledge the financial support from *El Patrimonio Autónomo Fondo Nacional de Financiamiento para la Ciencia, la Tecnología y la Innovación Francisco José de Caldas* (project: CD 111580863338, CT FP80740-173-2019).

[1] Gaixia Xu, Shuwen Zeng, Butian Zhang, Mark T. Swihart, Ken-Tye Yong, and Paras N. Prasad, *New generation Cadmium-free quantum dots for biophotonics and nanomedicine*, Chem. Rev. **116**, 12234-12327 (2016). DOI: 10.1021/acs.chemrev.6b00290

[2] Sungjee Kim, Brent Fisher, Hans-Jurgen Eisler, and Moungi Bawendi, *Type-II quantum dots: CdTe/CdSe (core/shell) and CdSe/ZnTe (core/shell) heterostructures*, J. Am. Chem. Soc. **125**, 1146611467 (2003). DOI: 10.1021/ja0361749

[3] Haiguang Zhao and Federico Rosei, *Colloidal quantum dots for solar technologies*, Chem. **3**, 229-258 (2017). DOI: 10.1016/j.chempr.2017.07.007

[4] Amira R. AbouElhamd, Khaled A. Al-Sallal, and Ahmed Hassan, *Review of core/shell quantum dots technology integrated into buildings glazing*, Energies **12**, 1058 (pp22) (2019). DOI: 10.3390/en12061058

[5] Shuang Jiao, Qing Shen, Ivn Mora-Sero, Jin Wang, Zhenxiao Pan, Ke Zhao, Yuki Kuga, Xinhua Zhong, and Juan Bisquert, *Band engineering in core/shell ZnTe/CdSe for photovoltage and efficiency enhancement in exciplex quantum dot sensitized solar cells*, ACS Nano **9**, 908915 (2015). DOI: 10.1021/nn506638n

[6] Tongqing Long, Jun Cao, and Zhong-Jie Jiang, *Predictable spectroscopic properties of type-II ZnTe/CdSe nanocrystals and electron/hole quenching*, Phys. Chem. Chem. Phys. **21**, 5824-5833 (2019). DOI: 10.1039/C9CP00026G

[7] Sreejith Kaniyankandy, S. Rawalekar, Sandeep Verma, and Hirendra N. Ghosh, *Ultrafast hole transfer in CdSe/ZnTe type II core-shell nanostructure*, J. Phys. Chem. C. **115**, 14281435 (2011). DOI: 10.1021/jp107531h

[8] Tiberius O. Cheche, Valentin Barna, and Yia-Chung Chang, *Analytical approach for type-II semiconductor spherical core-shell quantum dots heterostructures with wide band gaps*, Superlattices Microstruct. **60**, 475-486 (2013). DOI: 10.1016/j.spmi.2013.05.027

[9] A. Chafai, F. Dujardin, I. Essaoudi, and A. Ainane, *Energy spectrum of an exciton in a CdSe/ZnTe type-II core/shell spherical quantum dot*, Superlattices Microstruct. **101**, 40-48 (2017). DOI: 10.1016/j.spmi.2016.11.017

[10] A. Naifar, N. Zeiri, S. Abdi-Ben Nasrallah, and M. Said, *Optical properties of CdSe/ZnTe type II core shell nanostructures*, Optik **146**, 90-97 (2017). DOI: 10.1016/j.ijleo.2017.08.079

[11] A Chafai, I. Essaoudi, A. Ainane, F. Dujardin, and R. Ahuja, *ZnTe/CdSe type-II core/shell spherical quantum dot under an external electric field*, Mater. Devices **3**, 0504 (pp6) (2018). DOI: 10.23647/ca.md20180504

[12] E. J. Tyrrell and J. M. Smith, *Effective mass modeling of excitons in type-II quantum dot heterostructures*, Phys. Rev **84**, 165328 (pp12) (2011). DOI: 10.1021/acs.jpcc.5b02789

[13] Edward J. Tyrrell and Stanko Tomic, *Effect of correlation and dielectric confinement on $1S^{(e)}_{1/2}nS^{(h)}_{3/2}$ excitons in CdTe/CdSe and CdSe/CdTe type-II quantum dots*, J. Phys. Chem. C. **119**, 12720-12730 (2015). DOI: 10.1021/acs.jpcc.5b02789

[14] Fatih Koc and Mehmet Sahin, *The electronic and optical properties of an exciton, biexciton and charged excitons in CdSe/CdTe-based multi-shell type-II quantum dot nanocrystals*, Appl. Phys. A. **125**, 705 (pp9) (2019). DOI: 10.1007/s00339-019-3000-3

[15] V. A. Harutyunyan, *Nanospherical heterolayer in strong electrostatic field*, Appl. Nanosci. **2**, 339-344 (2012). DOI: 10.1007/s13204-012-0087-7

[16] Yuan Jian-Hui, Xie Wen-Fang, and He Li-Li, *Shallow donor impurity ground state in a GaAs/AlAs spherical quantum dot within an electric field*, Commun. Theor. Phys. **52**, 710-714 (2009). DOI: 10.1088/0253-6102/52/4/30

[17] M. Cristea, *Simultaneous effects of electric field, shallow donor impurity and geometric shape on the electronic states in ellipsoidal ZnS/CdSe core-shell quantum dots*, Physica E **103**, 300-306 (2018). DOI: 10.1016/j.physe.2018.06.019

[18] Radmila Kostic and Dusanka Stojanovic, *Electric field effect on the nonlinear and linear intersubband absorption spectra in CdTe/ZnTe spherical quantum dot*, J. Nanophotonics **6**, 061606 (pp14) (2012). DOI: 10.1117/1.JNP.6.061606

[19] V. Holovatsky, M. Chubrey, and O. Voitsekhivska, *Effect of electric field on photoionisation cross-section of impurity in multilayered quantum dot*, Superlattices Microstruct. **145**, 106642 (pp9) (2020). DOI: 10.1016/j.spmi.2020.106642

[20] V. A. Holovatsky and I. B. Bernik, *Effect of magnetic and electric fields on optical properties of semiconductor spherical layer*, Semicond. Phys. Quantum Electron. Optoelectron. **17**, 7-13 (2014). DOI: 10.15407/spqeo17.01.007

[21] V. A. Holovatsky, M. Ya. Yakhnevych, and O. M. Voitsekhivska, *Optical properties of $GaAs/Al_xGa_{1-x}As/GaAs$ quantum dot with off-central impurity driven by electric field*, Condens. Matter Phys. **21**, 13703 (pp9) (2018). DOI: 10.5488/CMP.21.13703

[22] Mehmet ahin, Sedat Nizamoglu, A. Emre Kavruk, and Hilmi Volkan Demir, *Self-consistent computation of electronic and optical properties of a single exciton in a spherical quantum dot via matrix diagonalization method*, J. Appl. Phys. **106**, 043704 (pp5) (2009). DOI: 10.1063/1.3197034

[23] N. V. Tkach, V. A. Holovatsky, and O. N. Voitsekhivska, *On the spectra of electrons and holes in an open spherical nanoheterostructure (through the example of $GaAs/AlxGa_{1-x}As/GaAs$)*, Semiconductors 34, 602-

606 (2000). DOI: 10.1134/1.1188032

[24] Liangliang Lu, Wenfang Xie, and Zhewei Shu, *Combined effects of hydrostatic pressure and temperature on nonlinear properties of an exciton in a spherical quantum dot under the applied electric field*, Physica B **406**, 3735-3740 (2011). DOI: 10.1016/j.physb.2011.06.08

[25] Ahmet Emre Kavruk, *A detailed investigation of electronic and optical properties of single exciton in* $GaAs/Al_xGa_{1-x}As/GaAs/Al_yGa_{1-y}As$ *multi-shell quantum dot*, Philos. Mag. **98**, 3109-3125 (2018). DOI: 10.1080/14786435.2018.1519260

[26] Marco Califano, Alberto Franceschetti, and Alex Zunger, *Lifetime and polarization of the radiative decay of excitons, biexcitons, and trions in CdSe nanocrystal quantum dots*, Phys. Rev. B **75**, 115401 (pp7) (2007). DOI: 10.1103/PhysRevB.75.115401

[27] Benito Alen, Jose Bosch, Daniel Granados, Juan Martinez-Pastor, Jorge M. Garcia, and Luisa Gonzalez, *Oscillator strength reduction induced by external electric fields in self-assembled quantum dots and rings*, Phys. Rev. B **75**, 045319 (pp7) (2007). DOI: 10.1103/PhysRevB.75.045319

[28] Nikita V. Tepliakov, Mikhail Yu. Leonov, Alexander V. Baranov, Anatoly V. Fedorov, and Ivan D. Rukhlenko, *Quantum theory of electroabsorption in semiconductor nanocrystals*, Opt. Express **24**, 251452 (pp6) (2016). DOI:10.1364/OE.24.000A52

[29] Sandeep Verma, Sreejith Kaniyankandy, and Hirendra N. Ghosh, *Charge separation by indirect bandgap transitions in CdS/ZnSe type-II core/shell quantum dots*, J. Phys. Chem. C **117**, 1090110908 (2013). DOI: 10.1021/jp400014j

[30] Xuedan Ma, Alf Mews, and Tobias Kipp, *Determination of electronic energy levels in type-II CdTe-core/CdSe-shell and CdSe-core/CdTe-shell nanocrystals by cyclic voltammetry and optical spectroscopy*, J. Phys. Chem. C **117**, pp. 1669816708 (2013). DOI: 10.1021/jp404556b

[31] Clare E. Rowland, Marc Currie, Kimihiro Susumu, Eunkeu Oh, Gary Kushto, Alexander L. Efros, Alan H. Huston, and James B. Delehanty, *Effects of shell thickness on the electric field dependence of exciton recombination in CdSe/CdS core/shell quantum dots*, Opt. Mater. Express **7**, 1871 (pp11) (2017). 10.1364/OME.7.001871

[32] A. Chafai, F. Dujardin, I. Essaoudi, and A. Ainane, *Energy spectrum of an exciton in a CdSe/ZnTe type-II core/shell spherical quantum dot*, Superlattices Microstruct. **101**, 40-48 (2017). DOI: 10.1016/j.spmi.2016.11.017

[33] T. O. Cheche and Y-.C. Chang, *Efficient modeling of optical excitations of colloidal core-shell semiconductor quantum dots by using symmetrized orbitals*, J. Phys. Chem. A, **122**, 9910-9921 (2018). DOI: 0.1021/acs.jpca.8b09758

## DECLARATION OF COMPETING INTEREST

The authors declare that they have no known competing financial interests or personal relationships that could have appeared to influence the work reported in this paper.

## CREDIT AUTHOR STATMENT

V. A. Holovatsky: Conceptualization, Methodology, Software, Validation, Formal analysis, Investigation, Writing - original draft, Writing - review & editing, Visualization, Supervision.

M. V. Chubrei: Software, Validation, Formal analysis, Investigation, Writing - original draft.

C. A. Duque: Validation, Formal analysis, Resources, Data curation, Writing - review & editing.